ELSEVIER

Physica B 204 (1995) 14–19

PHYSICA B

Ultrasonic modulation of multiply scattered light

W. Leutz[1], G. Maret*,[2]

High Magnetic Field Laboratory, Max-Planck-Institut für Festkörperforschung, and Centre National de la Recherche Scientifique, B.P. 166, F-38042 Grenoble Cedex 9, France

Abstract

We report the first observation of ultrasonic modulation of multiple light scattering speckles. The modulation at $f_a = 2$ MHz of the temporal field autocorrelation function $\langle E(0)E^*(t)\rangle$ of the light scattered from concentrated aqueous suspensions of polystyrene beads was measured. In addition, when using $f_a = 27$ MHz, the light intensity spectra measured with a Fabry–Perot interferometer show four inelastic peaks at f_a and $2f_a$ from the principal Rayleigh peak. The modulation amplitudes obtained from both techniques were found to increase with the ultrasonic amplitude and to vary with the mean free path of light in agreement with our simple model.

1. Introduction

In recent years dynamic multiple scattering of light (DMLS) in disordered inhomogeneous media has become a subject of great interest. Many experiments were performed on concentrated suspensions of colloidal particles such as polystyrene beads. The Brownian motion of scatterers gives rise to rapid temporal phase shifts of the multiply scattered light. By measuring the temporal autocorrelation function of the scattered light intensity, the size and dynamics of the scatterers can be determined on much shorter time- and length scales than in the single scattering regime [1–3]. Therefore DMLS also allows the determination of the short-time self-diffusion constant of spheres with interparticle correlations in very concentrated suspensions (strong multiple scattering regime) [4]. Another, example of DMLS is the investigation of the collective motion of scatterers in shear flow [5, 6].

In this paper we discuss the effect of periodic motion on DMLS in the transmission geometry: In addition to Brownian motion the scatterers undergo a collective motion generated by ultrasound. We outline a simple model for this effect. To test this model we have performed two different experiments: First we measured the modulation of the temporal field autocorrelation function $\langle E(0)E^*(t)\rangle$ at an ultrasonic frequency of about 2 MHz. Then we made intensity spectra of the scattered light using a Fabry–Perot interferometer at an ultrasonic frequency of 27 MHz. Both experiments were performed as a function of the ultrasonic amplitude and the transport mean free path l^* of the multiply scattered photons. An optical calibration of the ultrasonic amplitude using the Raman–Nath effect [7, 8] allows us to compare our measured results with our simple model.

2. Theoretical considerations

2.1. Dynamic correlation function

Let us consider point-like scatterers undergoing Brownian motion and collective motion generated by

* Corresponding author.
[1] Present address: Institute of Applied Physics, Sidlerstr. 5, CH-3012 Bern, Switzerland.
[2] Present address: Inst. Charles Sadron, CNRS, 6, rue Boussingault F-67083 Strasbourg-Cedex, France.

SSDI 0921-4526(94)00238-X

ultrasound. We assume that the scattering mean free path l of light between successive scatterers along a scattering path is much larger than the wavelength λ_0 of light and that there are no correlations between the different random paths (weak scattering approximation). Then, for paths of length s much larger than l, the autocorrelation function $G_1(t)$ of the electrical field component of the scattered light is obtained by summing over different s:

$$G_1(t) = \langle E(0)E^*(t)\rangle = \int_l^\infty P(s)\langle E_s(0)E_s^*(t)\rangle \, \mathrm{d}s. \tag{1}$$

E_s is the electrical field component of the light scattered along a path of length s. The distribution function $P(s)$ is the fraction of the incident intensity scattered into paths of length s. Assuming that Brownian (subscript B) and ultrasonic (U) motion are independent, the average field correlation function along paths of length s is given by $\langle E_s(0)E_s^*(t)\rangle_B \langle E_s(0)E_s^*(t)\rangle_U$.

For Brownian motion we have [1, 2] with the single particle relaxation time $\tau_0 = 1/Dk_0^2$ (D: particle diffusion constant; k_0: light wave vector):

$$\langle E_s(0)E_s^*(t)\rangle_B = \exp\left(-\frac{2ts}{\tau_0 l}\right). \tag{2}$$

The autocorrelation function for the ultrasonic motion along a path with s/l scatterers is

$$\langle E_s(0)E_s^*(t)\rangle_U = \left\langle \exp\left[-\mathrm{i}\sum_{j=1}^{s/l}\Delta\phi_j(t)\right]\right\rangle \tag{3}$$

with the temporal phase shift due to the longitudinal ultrasound with amplitude A, frequency ω_a and wave vector $\boldsymbol{k}_a$

$$\sum_{j=1}^{s/l}\Delta\phi_j(t) = \sum_{j=1}^{s/l}\boldsymbol{k}_j(\Delta\boldsymbol{r}_{j+1,j}(t) - \Delta\boldsymbol{r}_{j+1,j}(0)). \tag{4}$$

$\Delta\boldsymbol{r}_{j+1,j}(t)$ is the distance between two successive scatterers at $\boldsymbol{r}_j$ and $\boldsymbol{r}_{j+1}$:

$$\Delta\boldsymbol{r}_{j+1,j}(t) = (\boldsymbol{r}_j + A\sin[\boldsymbol{k}_a\cdot\boldsymbol{r}_j - \omega_a t]) - (\boldsymbol{r}_{j+1} + A\sin[\boldsymbol{k}_a\cdot\boldsymbol{r}_{j+1} - \omega_a t]). \tag{5}$$

$\boldsymbol{k}_j$ is the light wave vector after the jth scattering event.

The $\Delta\phi_j(t)$ are independent variables with a gaussian distribution of variance $\langle\Delta\phi_j^2(t)\rangle$ (central limit theorem). For ultrasonic displacements much smaller than the light wavelength ($k_0A \ll 1$) we retain only the first cumulant:

$$\langle E_s(0)E_s^*(t)\rangle_U = \left\langle \exp\left[-\frac{\Delta\phi_j^2(t)}{2}\right]\right\rangle^{s/l} \approx \exp\left[-\frac{s}{l}\frac{\langle\Delta\phi_j^2(t)\rangle}{2}\right]. \tag{6}$$

$\langle\Delta\phi_j^2(t)\rangle$ is an average over the angles Θ_j between $\boldsymbol{k}_a$ and $\boldsymbol{k}_j$ and over all ultrasonic phases $\boldsymbol{k}_a\boldsymbol{r}_j$. For point-like scatterers Θ_j and $\boldsymbol{r}_j$ are independent, and after some algebra we obtain

$$\langle\Delta\phi_j^2(t)\rangle = (4k_0A)^2\sin^2\left[\frac{\omega_a t}{2}\right] \times \underbrace{\left\langle \sin^2\left[\boldsymbol{k}_a\boldsymbol{r}_j - \frac{\omega_a t}{2}\right]\right\rangle_{rj}}_{1/2} \times \underbrace{\left\langle \sin^2\left[\frac{k_a l}{2}\cos\Theta_j\right]\cos^2\Theta_j\right\rangle_{\Theta_j}}_{\alpha}.$$

We obtain

$$\alpha = \frac{1}{6} - \frac{\cos[k_a l]}{(k_a l)^2} + \frac{\sin[k_a l]}{(k_a l)^3} - \frac{\sin[k_a l]}{2(k_a l)}. \tag{7}$$

α is a function of the ultrasonic wavelength $\lambda_a = 2\pi/k_a$ and the mean free path l of the light and is shown as the continuous line in Fig. 6. α has a maxima if l is half a multiple of $\lambda_a = 2\pi/k_a$. In this case the oscillatory motions of two successive scatterers have opposite phases and therefore their relative displacements have a maxima. For integral multiples the motions are in phase and $\langle\Delta\phi_j^2(t)\rangle$ has a minima. The total field correlation function can be written as follows:

$$G_1(t) = \int_{s=l}^\infty P(s)\exp\left[-\frac{2s}{l} \times\left(\frac{t}{\tau_0} + (k_0A)^2(1-\cos[\omega_a t])\alpha\right)\right]\mathrm{d}s. \tag{8}$$

We consider the transmission of light through a slab of thickness L and of infinite extent. For uniform light incident from an extented plane source and collected from a point on the other side of the slab, we finally obtain for the field correlation function [9]:

$$G_1(t) = \frac{\sqrt{6\left(\frac{L}{l}\right)^2\left(\frac{t}{\tau_0} + (k_0A)^2(1-\cos[\omega_a t])\alpha\right)}}{\sinh\sqrt{6\left(\frac{L}{l}\right)^2\left(\frac{t}{\tau_0} + (k_0A)^2(1-\cos[\omega_a t])\alpha\right)}}. \tag{9}$$

$G_1(t)$ is a decaying function due to the Brownian motion of the scatterers superimposed with a modulation of the ultrasonic frequency ω_a. For scatterers of finite size (comparable or larger than λ_0), the distance l^*, over which the direction of propagation of light is randomized, becomes

larger than l. In this case, the evaluation of α is not straightforward.

2.2. Intensity spectra

The intensity spectrum, which can be measured with a Fabry–Perot interferometer, is the Fourier transform of $G_1(t)$ (Wiener–Khintchin theorem):

$$I_n = \frac{1}{T}\int_0^T \cos[n\omega_a t]\,\frac{\sqrt{b(1-\cos[\omega_a t])}}{\sinh[\sqrt{b(1-\cos[\omega_a t])}]}\,\mathrm{d}t$$

$$(T = 2/\omega_a) \tag{10}$$

with $b = 6(L/l)^2(k_0 A)^2\alpha$. In particular I_1/I_0, which is the measured quantity in our experiment, can be approximated by

$$I_1/I_0 = 8.211\times10^{-2}b - 4.584\times10^{-3}b^2 + 1.78\times10^{-4}b^3 - 3.398\times10^{-6}b^4. \tag{11}$$

3. Experimental

We studied the ultrasonic modulation of multiply scattered light with two different experimental procedures:
1. the temporal field correlation function at an ultrasonic frequency of 2.17 MHz,
2. Intensity spectra with a Fabry–Perot at an ultrasonic frequency of 27.3 MHz as a function of the ultrasonic amplitude and of the transport mean free path l^* of light.

In all experiments we used aqueous suspensions of 0.25 μm polystyrene bead with $l^* = 3l$ as samples. Particle volume fractions and l^* values are summarized in Table 1.

Table 1
Transport mean free paths l^* as measured for different polystyrene bead (diameter: $d = 0.25$ μm) solid fracitons ρ in the experiments with the correlator and the Fabry–Perot. The l^* values are, within the 10%- error bars, consistent with those calculated from Mie scattering [4]

Correlator			Fabry–Perot		
ρ	l^* (μm)	l^*/λ_a	ρ	l^* (μm)	l^*/λ_a
1.248%	234	0.34	15.4%	17	0.31
0.828%	304	0.45	7.3%	29	0.53
0.624%	370	0.54	3.8%	59	1.09
0.417%	571	0.84	2.5%	84	1.55
0.275%	770	1.1	1.88%	111	2.05

3.1. Calibration of the ultrasonic amplitude

In order to compare our data with the model, we have calibrated the ultrasonic amplitude in water optically using the Raman–Nath effect [8]. A refractive index grating is set up by an ultrasonic wave in a transparent fluid giving rise to a characteristic light intensity diffraction pattern. The diffraction angle depends on the ultrasonic wavelength and the diffracted intensity on the acoustic amplitude [7]. For light incidence normal to the direction of the ultrasonic propagation, the intensity I_k of the diffraction order k as compared to the nondiffracted intensity is a squared Bessel function $|J_k[v]|^2$ of order k of the Raman–Nath parameter v.

$v = (\partial n/\partial p)_{ad}\rho\omega_a c_s k_0 L A$ is proportional to the ultrasonic amplitude A. $(\partial n/\partial p)_{ad} = 1.466\times10^{-10}$ N/m^2, $\rho = 10^3$ kg/m^3 and $c_s = 1480$ m/s are the adiabatic piezo-optical coefficient, the density and the velocity of sound of water, respectively.

A parallel light beam ($\lambda_0 = 514.5$ nm) from an argon laser is sent through a rectangular glass cell (thickness $L = 5$ mm, width 20 mm) filled with water. The ultrasound passes through the sample perpendicular to the optical axis. To obtain a predominantly propagative wave, the ultrasound is absorbed by a neoprene absorber inserted into the cell at the opposite side of the transducer. A photodiode measures the light intensities of the zeroth and first diffraction order for different ultrasonic driver voltages V. Then we get the Raman–Nath parameter v by curve fitting, which is also proportional to V, and therefore the calibration curve between A and V.

3.2. Measurement of the field autocorrelation function

The experimental setup to measure $\langle E(0)E^*(t)\rangle$ in the transmission geometry is shown in Fig. 1. The incident laser beam ($\lambda_0 = 514.5$ nm, Laser power: 600 mW) of 2 mm diameter impinged on the same cell used for the Raman–Nath calibration. A 120 mm focal length lens collected the scattered laser light into a glass fiber guiding it to a photomultiplier (PM). An electronic correlator determined $\langle E(0)E^*(t)\rangle$ by photon counting. Two pinholes, one in front of the lens and the other in front of the glass fiber, make sure that somewhat less than one speckle spot (or one coherence area) is observed. A ceramic transducer, which is fixed at the outside of the scattering cell, generates ultrasound with a frequency of 2.17 MHz perpendicular to the incident laser beam. The correlator sampling time is set at 60 ns to achieve sufficient time resolution. Polystyrene bead suspensions with 5 different solid fractions ρ were used. Their transport mean free path l^* of light is estimated by measuring $G_1(t)$ without ultrasound and curve fitting with Eq. (9)

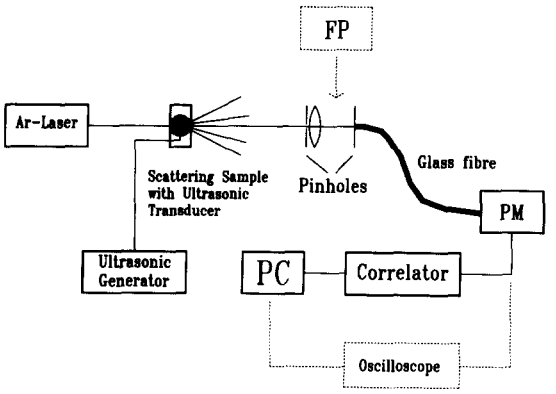

Fig. 1. The arrangement for the dynamical light scattering experiment with the correlator or with the Fabry–Perot interferometer (dotted line).

(Table 1). The l^* values agree, within a 10% rms-error, with those calculated from Mie scattering.

3.3. Measurement of the intensity spectra

Fig. 1 shows the experimental setup to record the spectra of multiply scattered light with a Fabry–Perot interferometer. The scattered argon laser light is focused onto a pinhole (diameter: 50 μm). A second lens (not shown) causes the light which is parallel to pass through the Fabry–Perot. At its exit, a collimator lens (not shown) focuses the light through a second pinhole (diameter: 50 μm) into a glass fiber, which guides it to a photomultiplier. The spectra are observed using a sampling oscilloscope which is triggered by the peak of the Rayleigh line (elastic scattering). The two mirrors (Reflectivity: 99.3%) in the Fabry–Perot interferometer are separated by 15 cm, providing a free spectral range of 1 GHz. The resolution of the Fabry–Perot was about 12 MHz. The ultrasound (frequency: 27.3 MHz) is generated by a $LiNbO_3$-Transducer (Size: 2 mm × 2 mm) positioned inside the scattering cell of thickness $L = 2$ mm. The 5 samples of different solid fractions ρ of aqueous polystyrene bead suspensions used in this experiment had smaller values of l^*, as shown in Table 1.

4. Results

4.1. Ultrasonic modulation of $G_1(t)$

Fig. 2 shows measured autocorrelation functions $G_1(t)$ for an aqueous polystyrene bead suspension with $l^* = 370$ μm modulated by an ultrasonic wave with 2.17 MHz frequency ($\lambda_a = 682$ μm) at two different ultrasonic amplitudes. $G_1(t)$ has a modulation period of 0.46 μs according to the ultrasonic frequency. The envelope of the curves decays and the ultrasonic modulation is damped due to Brownian motion. From a fit using Eq. (9)

$$G_1(t) = \frac{\sqrt{at + b(1 - \cos[\omega_a t])}}{\sinh\sqrt{at + b(1 - \cos[\omega_a t])}}$$

we obtain the parameter a due to Brownian motion and the dimensionless ultrasonic modulation amplitude b of $G_1(t)$. Fig. 3 shows b as a function of A. From a parabolic fit through b we obtain the coefficient $\gamma = b/A^2$ which equals $6(k_0 L/l)^2\ \alpha$ according to Eqs. (9) and (10).

In order to obtain α, which describes the l-dependence of the average phase-shift $\langle \Delta_j^2(t) \rangle$ of light per scattering event we evaluated $\gamma/6(k_0 L/l)^2$ for 5 different solid fractions ρ shown in Table 1. In Fig. 6, α is plotted versus $k_a l$ (fixed ultrasonic wave number k_a). α increases with l qualitively as predicted in our model.

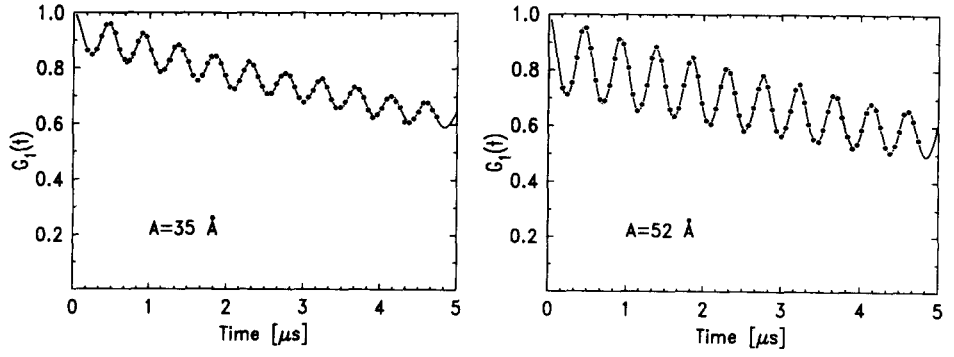

Fig. 2. Measured $G_1(t)$ (●) for multiply scattered light at two different ultrasonic amplitudes A ($f_a = 2.17$ MHz). The continuous line is the fit with Eq. (9). The ultrasonic modulation is damped due to Brownian motion of the scatterers. $l^* = 370$ μm.

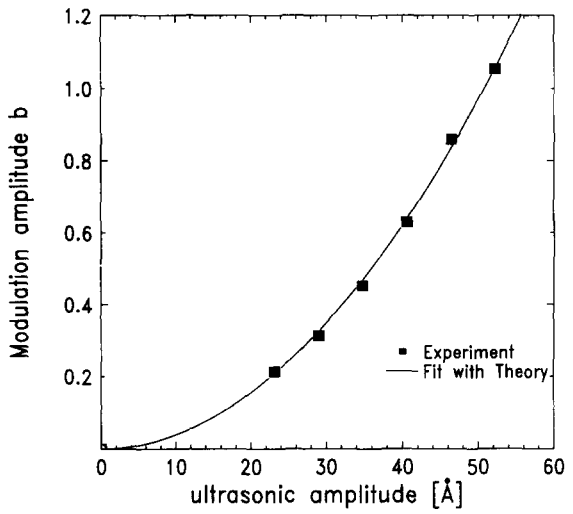

Fig. 3. The modulation parameter b of $G_1(t)$ increases with the ultrasonic amplitude.

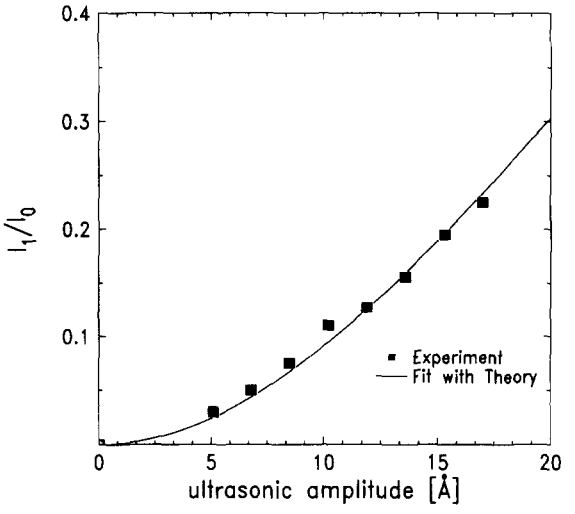

Fig. 5. The intensity ratios I_1 and I_0 as a function of the ultrasonic amplitude A.

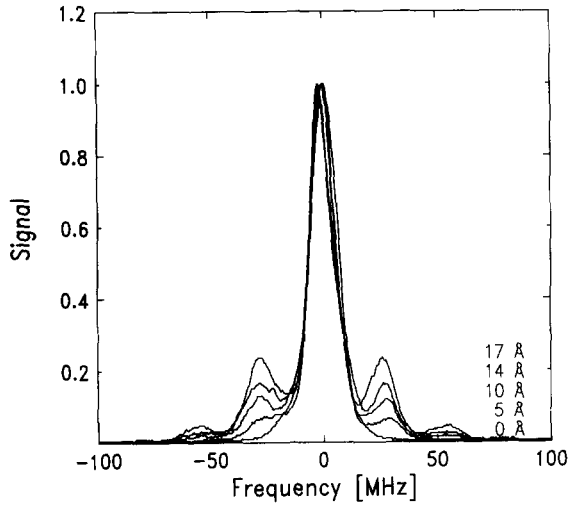

Fig. 4. Intensity spectra of multiply scattered light at different ultrasonic amplitudes ($f_a = 27.3$ MHz). They show peaks at f_a and $2f_a$ from the Rayleigh peak. $l^* = 17$ μm.

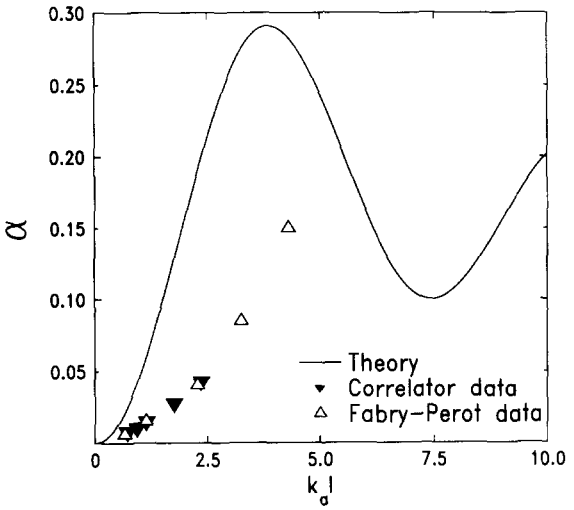

Fig. 6. α as a function of the transport mean free path l with the ultrasonic wave vector k_a fixed.

4.2. *Intensity spectra*

In Fig. 4, five spectra, taken at different ultrasonic amplitudes for a sample with $l^* = 17$ μm, show peaks displaced by the single (27.3 MHz) and by the double ultrasonic frequency from the Rayleigh peak. For the analysis we subtracted the spectra from the spectrum without ultrasound because the ultrasonic peaks sit on the 'foot' of the Rayleigh peak. Then we estimated the relative height I_1/I_0 of the singly displaced peaks. In Fig. 5 I_1/I_0 is plotted versus the ultrasonic amplitude A. From a fit with Eq. (11), using $b = \gamma A^2$, through the data we get the fit parameter $\gamma = 6(k_0 L/l)^2 \alpha$. We estimated α for 5 samples with different l (Table 1: $l^* = 3l$). α increases with $k_a l$ as plotted in Fig. 6.

5. Discussion and conclusions

In this paper we demonstrate the modulation of multiply scattering speckle patterns by propagative longitudinal ultrasound using two different experiments. The measured field correlation function $G_1(t)$ has a modulation period according to the applied ultrasonic freqeuency of 2.17 MHz and decays with time because of Brownian motion of the scatterers. The modulation amplitude of $G_1(t)$ increases with the square of the ultrasonic amplitude. Intensity spectra taken with a Fabry–Perot interferometer show four ultrasound induced peaks shifted by the single (I_1; $f_a = 27.3$ MHz) and by the double ultrasonic frequency (I_2) from the Rayleigh peak (I_0). The relative peak height I_1/I_0 at f_a grows with the ultrasonic amplitude. Both experiments are done for various transport mean free paths $l^* = 3l$ but fixed ultrasonic wave vector k_a.

We determined α which describes the average phase-shift on the length scale l as a function of $k_a l$. Both experimental data sets fit well together and increase with $k_a l$ as shown in Fig. 6. The values for α are smaller than predicted by our model for point-like scatterers where no correlations between successive scattering steps occur ($l^* = l$). But in our experiments we used scatterers of dimensions comparable with the light wavelength (Mie scattering) and therefore $l^* > l$ should be the characteristic length scale for α. According to Mie theory, we calculated that the direction of propagation of light is randomized over a distance $l^* = 3l$. The evaluation of α is not straightforward and should be determined in this case by computer simulations.

For our experiments we have independently measured the ultrasonic amplitude (in pure water with the Raman–Nath effect) and the transport mean free path l^*. For l^*, we find good agreement between theory and experiment. By solving the equation of oscillatory motion of a sphere in a viscous fluid, we estimated that the displacements of the scatterers almost entirely follow the ultrasonic amplitudes. The damping of the ultrasonic wave in water (absorption length for 30 MHz: 4 cm) and ultrasound scattering in the polystyrene bead suspension (scattering mean free path of ultrasound > 100 m) can be neglected. To get an ideal harmonic progressive wave, we put a rippled absorber made of damping neoprene in our scattering cell which reduces backscattering from the walls. Incoherently scattered ultrasound from the absorber could superimpose on the incoming coherent part resulting in a nonsinusoidal ultrasonic wave. Their spatial random distributed amplitudes could reduce α. Since this incoherent part should strongly depend on frequency, the observed superposition of the data sets from two different experiments suggests that this effect is indeed negligible.

In summary, the observed acoustic modulation of multiple scattering speckles can be qualitatively explained by a simple model. However, the experimental determination of all relevant parameters reveals quantitative differences with this model. This may originate from the use of point-like scatterers in the model, or from an underestimate of the effect of incoherent ultrasound. An extension of our model to Mie scatterers would therefore be very significant. One could also attempt to generate a more ideal coherent progressive ultrasonic wave. Notwithstanding, this work reveals, in principle, the possibility to measure amplitudes of progressive harmonic ultrasound in optically turbid media with conventional light scattering equipment.

References

[1] G. Maret and P.E. Wolf, Z. Phys. B 65 (1987) 409.
[2] D.J. Pine, D.A. Weitz, G. Maret, P.E. Wolf, E. Herbolzheimer and P.M. Chaikin, in: Classical Wave Localisation, ed. P. Sheng (World Scientific, London, Singapore, 1989).
[3] M. Rosenbluh, M. Hoshem, I. Freund and M. Kaveh, Phys. Rev. Lett. 58 (1987) 2754.
[4] S. Fraden and G. Maret, Phys. Rev. Lett. 65 (1990) 512.
[5] X.L. Wu, D.J. Pine, P.M. Chaikin, J.S. Huang and D.A. Weitz, J. Opt. Soc. Am. B 7 (1990) 15.
[6] D. Bicout, E. Akkermans and R. Maynard, J. Phys. 1 (1991) 471.
[7] P. Debye and F.W. Sears, Proc. Nat. Acad. Sci. Wash. 18 (1932) 409.
[8] C.V. Raman and N.S.N. Nath, Proc. Indian Acad. Sci. 2 (1935) 406, 413.
[9] D.J. Pine, D.A. Weitz, P.M. Chaikin and E. Herbolzheimer, Phys. Rev. Lett. 60 (1988) 1134.